Contents lists available at ScienceDirect

# **Journal of Catalysis**

journal homepage: www.elsevier.com/locate/jcat



# Direct conversion of dimethyl ether and CO to acetone via coupling carbonylation and ketonization



Ziqiao Zhou a,b,1, Hongchao Liu a,1, Youming Ni a, Fuli Wen a,b, Zhiyang Chen a,b, Wenliang Zhu a,\*, Zhongmin Liu a,b,\*

#### ARTICLE INFO

Article history Received 4 November 2020 Revised 2 March 2021 Accepted 8 March 2021 Available online 13 March 2021

Keywords: Dimethyl ether Acetone Carbonylation Ketonization H-mordenite

#### ABSTRACT

Acetone is currently produced by large amount of propylene and benzene, and its synthesis from a cheap and non-petroleum material has not yet been reported. Here, we present a new method for acetone production, which involves the carbonylation of dimethyl ether (DME) to methyl acetate and its subsequent ketonization to acetone over pyridine-modified H-mordenite. This convenient approach offers an acetone selectivity of 73% (CO<sub>2</sub> excluded) and a DME conversion of 100% at 553 K. Spectral and isotopic studies revealed that the ketonization of methyl acetate was promoted by carbonylation, while the formation of a ketene intermediate was demonstrated by the formation of CH<sub>2</sub>DCOOD and two types of pyrones. A ketene-based ketonization mechanism was also proposed based on the kinetic isotope effect of CH<sub>2</sub>=13C=0, indicating that the acetyl moiety contributed to the acyl part of acetone, while the ketene moiety was responsible for the alkyl part of acetone and the generation of CO<sub>2</sub>.

© 2021 Elsevier Inc. All rights reserved.

# 1. Introduction

Acetone is a bulk chemical, widely used as solvent and raw material for the production of ketene, acetic anhydride, chloroform, iodoform, isopropanol, etc. However, acetone production is currently based on petroleum industry using large amounts of propylene, pointing out that novel preparation methods based on non-petroleum resources need to be developed. Therefore, in this study, we considered using dimethyl ether (DME) as an alternative substrate for the direct production of acetone. To the best of our knowledge, this preparation method has not been reported so far.

DME is an important platform compound in  $C_1$  chemistry, as it can be used to produce a wide range of materials and liquid fuels. DME can be produced on a large scale from coal, natural gas, or even biomass, making it an ideal alternative to petroleum. [1-3] The carbonylation of DME has received great attention in the last decade due to its potential application for ethanol synthesis, while it has also been used for the formation of useful oxygenates such as acetic acid and methyl acetate. The zeolite-catalyzed DME carbonylation was first reported by Fujimoto et al. [4], while Hmordenite (H-MOR) and H-ferrierite (H-FER) have also been applied with high selectivity [5,6]. Based on studies on the reaction mechanism of DME carbonylation over H-MOR [7-12], DME initially generates methoxy species via a methylation step. CO is then inserted to the methoxy species, forming acetyl species that finally react with DME, generating methyl acetate and methoxy species [8]. Additional studies have demonstrated that DME carbonylation occurs preferably in the eight-membered ring (8MR) side pocket of H-MOR [8,10,13], whereas the formation of hydrocarbons (coke) leading to catalyst deactivation is favored in the 12MR main channel of H-MOR [10,13] and can be suppressed through ionic exchange [14,15], pyridine modification [16], and selective acid removal [17] strategies.

Ketonization involves the formation of ketones by carboxylic acids and esters and has received particular attention due to its application in the removal of carboxylic components in biomass conversion [18-20]. Ketonization reaction is also a key step in the direct conversion of DME to acetone. To date, the ketonization of carboxylic acids has been successfully performed over various metal oxides [21,22] and zeolites [19,20]. Recently, there are several detailed studies about metal oxide-catalyzed ketonization from Wang et al. [23,24] and Almutairi et al. [25]. For zeolitecatalyzed ketonization, an earlier study showed that acetyl species

a National Engineering Laboratory for Methanol to Olefins, Dalian National Laboratory for Clean Energy, iChEM, Dalian Institute of Chemical Physics, Chinese Academy of Sciences Dalian 116023 PR China

<sup>&</sup>lt;sup>b</sup> University of Chinese Academy of Sciences, Beijing 100049, PR China

<sup>\*</sup> Corresponding authorsat: National Engineering Laboratory for Methanol to Olefins, Dalian National Laboratory for Clean Energy, iChEM, Dalian Institute of Chemical Physics, Chinese Academy of Sciences, Dalian 116023, PR China (Z. Liu).

E-mail addresses: wlzhu@dicp.ac.cn (W. Zhu), liuzm@dicp.ac.cn (Z. Liu).

<sup>&</sup>lt;sup>1</sup> These authors contributed equally.

could be formed over zeolite after adsorption of acylation agents (acetyl chloride, acetic acid, and acetic anhydride) and suggested that acetone and acetylene resulted from the reaction of propylene and ketene [26]. Recently, Crossley *et al.* highlighted the importance of acetyl species during the ketonization of acetic acid [27], suggesting that an enolized acetic acid can attack a surface acetyl species, yielding acetoacetic acid that subsequently decomposes to acetone and  $\rm CO_2$ . Although the formation of acyl species rather than carboxylate was expected during ketonization reactions over zeolite [19,28] and confirmed by NMR studies [29–31], additional intermediates, such as ketene [32–36], anhydride [37,38], and  $\beta$ -keto acid [19], have also been identified during ketonization over metal oxides. However, the formation of these intermediates, especially of ketene, has been particularly questioned [19,39].

In this study, a new method was developed for the direct synthesis of acetone via the carbonylation of DME to methyl acetate and its subsequent ketonization over pyridine-modified H-MOR (Py-H-MOR). The selectivity of acetone reached 73% (CO<sub>2</sub> excluded) with 100% DME conversion at 553 K, indicating that this method can be used for acetone production from a non-petroleum-based  $C_1$  molecule while offering a new approach to DME carbonylation. A ketene-based mechanism was also suggested for the reaction to elucidate the contribution of the surface acetyl species and ketene to the formation of acetone and CO<sub>2</sub>, thus providing a new perspective to ketonization over zeolites.

#### 2. Experimental section

#### 2.1. Materials

H-Beta (Si/Al  $\sim$  20), H-Y (Si/Al  $\sim$  4), H-ZSM-5 (Si/Al  $\sim$  20) and H-ZSM35 (Si/Al  $\sim$  17) zeolites were obtained from Nankai University Catalyst Ltd. in the H<sup>+</sup> form and used as received. MOR (Si/Al = 16) was obtained in the Na<sup>+</sup> form from YanChang-ZhongKe Catalyst Ltd. All zeolites were characterized by X-ray diffraction, X-ray fluorescence analysis as well as scanning electron microscopy (Fig. S1).

 $D_2O$  (99.99%) was purchased from Shanghai ANNAIJI Chemical Co. Ltd.. DME as a mixture with 95% Ar (Dalian GuangMing Gas.), CO ( $^{13}$ CO used in the isotopic experiment was purchased from Cambridge Isotope Laboratory Inc. 99.99%  $^{13}$ C,  $^{13}$ CO as a mixture with 50% He), and Ar were controlled by a mass flow controller (SLA5850, Brooks Instrument). The reaction pressure was maintained by a back pressure regulator (TESCOM). Methyl acetate, acetic acid, and acetic anhydride were carried by Ar through a bubbler. The partial pressure of the liquid supply was adjusted by the bubbler temperature. Ar used as carrier gas was also controlled by a mass flow controller (5850E, Brooks Instrument). The line connecting the bubbler to the reactor was heated to prevent the condensation of the reactant.

# 2.2. Catalyst preparation

For the preparation of H-MOR, Na-MOR was first calcined at 823 K for 4 h in air to remove residual templates.  $NH_4$ -MOR was then obtained through ion exchange upon treatment with a  $NH_4$ -NO<sub>3</sub> solution (1.0 mol  $L^{-1}$ , solution/zeolite mass ratio = 10) at 353 K for 2 h. The solution was then filtered, the obtained  $NH_4$ MOR was washed with deionized water, and the ion exchange process was repeated twice. After drying at 393 K overnight,  $NH_4$ -MOR was measured by X-ray fluorescence spectrometry (XRF) to ensure the complete  $Na^+$  removal. H-MOR was then obtained after calcination of  $NH_4$ -MOR at 773 K for 3 h in flowing dry air.

Partially ion-exchanged MOR samples (NaNH<sub>4</sub>-MOR) were also prepared through a single ion exchange process of NH<sub>4</sub>-MOR (15 g)

using a NaNO<sub>3</sub> aqueous solution with concentrations of 0.005–0.1 mol  $\rm L^{-1}$  at 333 K for 3 h [40]. The obtained samples were then washed by deionized water, filtered, and dried at 393 K overnight. NaH-MOR was obtained similarly to H-MOR after the calcination of NaNH<sub>4</sub>-MOR.

To obtain pyridine-modified samples, catalysts (40–60 mesh) was loaded into a stainless fix-bed reactor (7 mm i.d.) and separated from quart sands by glass wool. Two K-type thermocouples were used to control and measure the reaction temperature. The catalyst was heated at 673 K for 2 h in flowing  $N_2$  (40 mL min $^{-1}$ ) to remove moisture and then cooled to 553 K for pyridine pretreatment.

Following an already reported process [16], Py-H-MOR was prepared by treating H-MOR with a 98%  $N_2/2\%$  pyridine mixture (30 mL min<sup>-1</sup>) at 553 K for 2 h, followed by treatment with 60 mL min<sup>-1</sup> pure  $N_2$  for 2 h to remove physically adsorbed pyridine. The temperature was then adjusted to the desired reaction temperature (453–653 K).

#### 2.3. Characterizations

The powder X-ray diffraction (XRD) patterns of the commercial samples were recorded using a PANalytical X'Pert PRO X-ray diffractometer with Cu K $\alpha$  radiation ( $\lambda$  = 0.154059 Å) at 40 kV and 40 mA from 5 to 60°. The elemental compositions of the zeolites were measured on a Philips Magix-601 X-ray fluorescence (XRF) spectrometer. The scanning electron microscopy (SEM) images of the zeolites were recorded on a Hitachi SU8020 SEM equipment.

The transmission infrared (IR) spectra of the NaH-MOR samples were recorded on a Bruker Tensor 27 instrument equipped with a vacuum system and a mercury cadmium telluride (MCT) detector. The samples were pressed in a self-supported wafer (~22.5 mg cm $^{-2}$ ) and heated to 623 K at 10 K min $^{-1}$  for 45 min under vacuum (10 $^{-2}$  Pa). After cooling to room temperature, the spectra were obtained at a resolution of 4 cm.

In situ diffuse reflectance infrared Fourier transform (DRIFT) spectroscopy was performed using a Bruker Tensor 27 instrument equipped with a diffuse reflectance attachment and a MCT detector. Py-H-MOR was smashed into powder and placed in a diffuse reflectance IR cell with a ZnSe window. Afterward, the catalyst powder was first heated at 473 K under vacuum for 2 h to remove moisture and then treated with flowing  $N_2$  (30 mL min $^{-1}$ ), passing through a methyl acetate bubbler, which was maintained at 313 K at the upper stream of the IR cell at ambient pressure for 2 h. The IR cell was then flushed with 30 mL min $^{-1}$  pure  $N_2$  for 1 h to remove residual gas and physically absorbed methyl acetate. After purification, the IR cell was filled with CO at a different pressure that was maintained by a back pressure regulator (XiongChuan). The *in situ* absorbance spectra were obtained by collecting 16 scans at 4 cm $^{-1}$  resolution 3 min after the pressure adjustment.

The temperature-programmed desorption (TPD) measurements were conducted in the reactor. After pyridine modification, the reactor was cooled to 473 K and the catalyst (0.4 g) was treated at ambient pressure for 2 h with 30 mL min<sup>-1</sup> Ar passing through a methyl acetate bubbler that was maintained at 313 K at the upper stream of the reactor. The catalyst was then treated at ambient pressure with pure Ar (50 mL min<sup>-1</sup>) for 1 h to remove physically absorbed methyl acetate. The desorption of products during the temperature rise was monitored by mass spectrometry (MS) (Pfeiffer, GSD320).

The products in the continuous flow reaction were analyzed by an on-line gas chromatograph (GC) (Agilent 7890B) equipped with a flame ionization detector connected with a HP-PLOT/Q capillary column (30 m  $\times$  0.53 mm  $\times$  40  $\mu m$ ), and a thermal-conductivity detector connected with a TDX-01 packed column. The line con-

necting the reactor outlet and the GC inlet was heated to avoid the condensation of the products.

The Guisnet's method [41] was also used to analyze the products deposited on the spent catalyst, which was dissolved in 20% HF, extracted with dichloromethane, and analyzed by GC–MS (Agilent 7890/5975C). The products collected from the isotopic experiment using <sup>13</sup>CO were collected by deionized water and a gas bag, and analyzed by GC–MS (Agilent 7890/5975C). The products obtained after the injection of deuterated water were analyzed by MS (Pfeiffer, GSD320).

All the above characterization experiments were performed separately and the data were collected when the acetone selectivity reached its maximum value. The conversion was calculated as follows:

$$Conversion(\%) = 100 \times \frac{F_{inlet} - F_{outlet}}{F_{inlet}} \tag{1} \label{eq:finlet}$$

where F<sub>inlet</sub> and F<sub>outlet</sub> represent the flow rate of the reactant at the reactor inlet and outlet, respectively.

Moreover, the selectivity of the products was calculated based on the moles of carbon:

$$Selectivity(C_nH_mO_l) = \frac{n \times N(C_nH_mO_l)}{\sum n \times N(C_nH_mO_l)} \eqno(2)$$

where  $N(C_nH_mO_l)$  represents the molar concentration of  $C_nH_mO_l$  and n is the number of carbons in  $C_nH_mO_l$ .

The molecular weight distribution of the product obtained using  $^{13}$ CO was correspondingly converted to probability distribution ( $P_n$ ) as follows:

$$P_n = \frac{I_n}{\sum I_n} \tag{3}$$

where n is the  $^{13}$ C amount in the molecule and  $I_n$  is the intensity of mass-spectrometry signal of the molecule.

#### 3. Results and discussion

#### 3.1. Coupling carbonylation and ketonization reactions

The coupling carbonylation of DME and the subsequent ketonization reaction were performed over various zeolites with different topologies and the results were compared (Fig. 1a). Specifically, only hydrocarbon products were observed over H-Beta, H-Y, and H-ZSM-5, whereas a methyl acetate selectivity of 17.3% was obtained over H-ZSM-35. However, when the reaction was performed over H-MOR, 35% acetic acid and a low amount of acetone (1.6%) was detected.

To limit the effect of the methanol-to-hydrocarbons (MTH) reaction over H-MOR, the catalyst was modified with pyridine (Py-H-MOR). H-MOR has two parallel 8MR and 12MR channels that are connected by an 8MR side pocket. The acid sites in the 12MR channel are responsible for the hydrocarbon formation [10,13] and can be deactivated by pyridine. Pyridine can also penetrate into the 8MR side pocket of H-MOR and desorb upon heating [42], as confirmed by IR measurements (Fig. S2). In particular, after treatment of H-MOR with pyridine, the peak corresponding to -OH stretching shifted from 3606 to 3585 cm<sup>-1</sup>, indicating the successful blockage of the acids in the 12MR channel. Similar results were obtained in earlier studies, where the IR peaks at 3616 and 3595 cm<sup>-1</sup> were attributed to the Brønsted acid sites in the 12MR channel and 8MR side pocket of H-MOR, respectively [43-45]. After pyridine modification, the selectivity of acetone over Py-H-MOR increased to 73%, while the hydrocarbon selectivity was significantly decreased to 2.2%. The time-on-stream of the

reaction is shown in Fig. 1b. Pyridine desorption was also considered by comparing the time-on-stream of 18 h of two reactions, which one of them possessed 18 h of pyridine desorption under the condition same to the reaction (except the addition of DME) before DME was introduced. The trend and the value of product selectivity were about same (Fig. S3). The similar time-on-stream of two reactions indicated that the effect of pyridine desorption was little.

In addition, it has been reported that the acid sites in the 8MR side pocket of H-MOR are active for DME carbonylation [8] and can catalyze the formation of acetic acid over H-MOR and Py-H-MOR. Comparison of the results obtained over H-MOR and Py-H-MOR revealed that the acetone formation was mainly catalyzed by the acid sites in the 8MR side pocket, while the formation of hydrocarbons was catalyzed by the acid sites in the 12MR channel, leading to lower acetone selectivity. Although the H-ZSM-35 zeolite also consists of an 8MR channel that can catalyze the carbonylation of DME [13], its 10MR channel promotes the MTH reaction and coke formation, and the water produced hydrolyzes DME, thus limiting the acetone production.

The effect of the reaction conditions, including the temperature, partial pressure of reactants (P), and contact time of the reactants with the catalyst was also investigated. As shown in Fig. 2a, the acetone selectivity was low at < 493 K, but increased significantly with increasing temperature, reaching a maximum at 573 K. In contrast, the selectivity of methyl acetate was rapidly reduced as the temperature increased, while at temperatures higher than 573 K, the formation of hydrocarbons  $(C_2^- + C_3^-)$  was observed. Carbonylation could take place easily at < 493 K, and methyl acetate was mainly formed, complying with already reported results [5,16]. Further increase of the reaction temperature (>493 K) favored the subsequent ketonization reaction, as confirmed by the detection of CO2 in the products, and an increasing acetone content was observed. Moreover, the molar flow rate ratio of CO<sub>2</sub>/acetone at 553 K was found to be about 1.1 (Fig. S4), i.e., close to the reported theoretical ratio  $(CO_2/\text{ketone} = 1)$  [19], further confirming the ketonization reaction. We also found that ketonization was more favored at about 550 K, as already reported in the literature [26,27]. Therefore, we concluded that the DME conversion to acetone could be achieved by adjusting the reaction temperature. However, it should be noted that temperatures higher than 573 K would activate side reactions, leading to the formation of hydrocarbons from DME or acetone and reducing the acetone selectivity [46,47].

The product selectivity was closely related with the reactants' partial pressure (P). Specifically, the DME conversion to acetone and acetic acid was higher with increasing  $P_{CO}$ , whereas the selectivity to methyl acetate was significantly reduced as  $P_{CO}$  increased (Fig. 2b). As expected, the opposite results were obtained with increasing DME pressure (Fig. 2c). Moreover, the maximum acetone selectivity was achieved at high  $P_{CO}/P_{DME}$  values, because the CO excess along with low DME content benefited the formation of acetone instead of methyl acetate.

Furthermore, in this study, the contact time was adjusted by the amount of catalyst loaded into the reactor, and the contact time variation indicated the change in the product distribution along the catalyst. Based on Fig. 2d, long contact times favored the acetone formation while reducing the selectivity of methyl acetate, whereas the acetic acid formation was almost independent from contact time, as a selectivity of about  $28.5\% \pm 1.5$  was observed throughout the experiment. Consequently, acetone was mainly formed by the ketonization of methyl acetate, while the contribution of the acetic acid ketonization was much smaller.

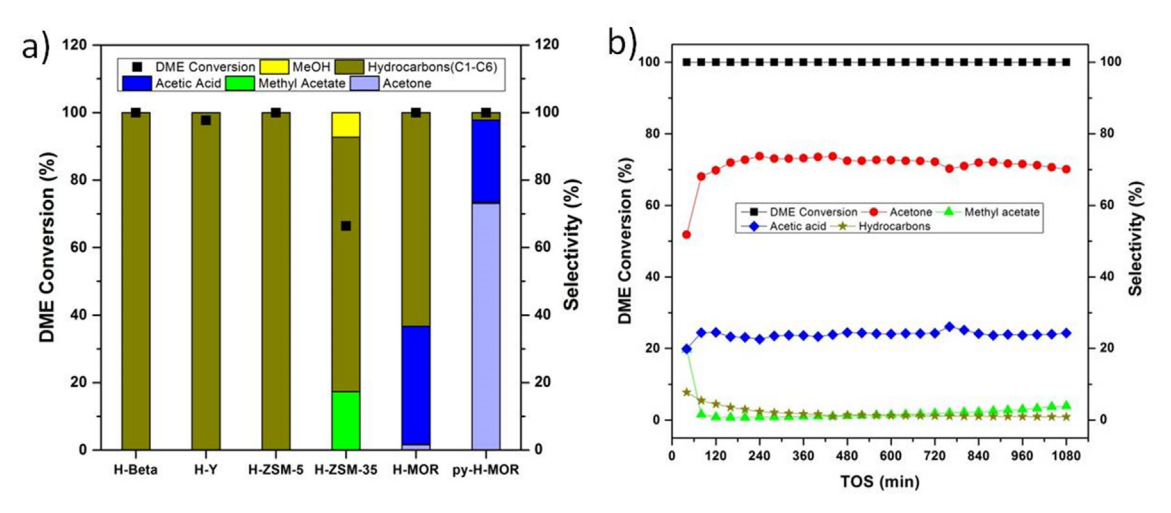


**Fig. 1.** (a) Results of the coupling carbonylation of DME and its subsequent ketonization reaction over commercially available zeolites and Py-H-MOR. (b) Time-on-stream of the reaction over Py-H-MOR. 553 K, 2 Mpa,  $P_{DME}$  = 56 kPa,  $P_{CO}$  = 888 kPa, total GHSV = 504 h<sup>-1</sup>. Ar was used as balancing gas.

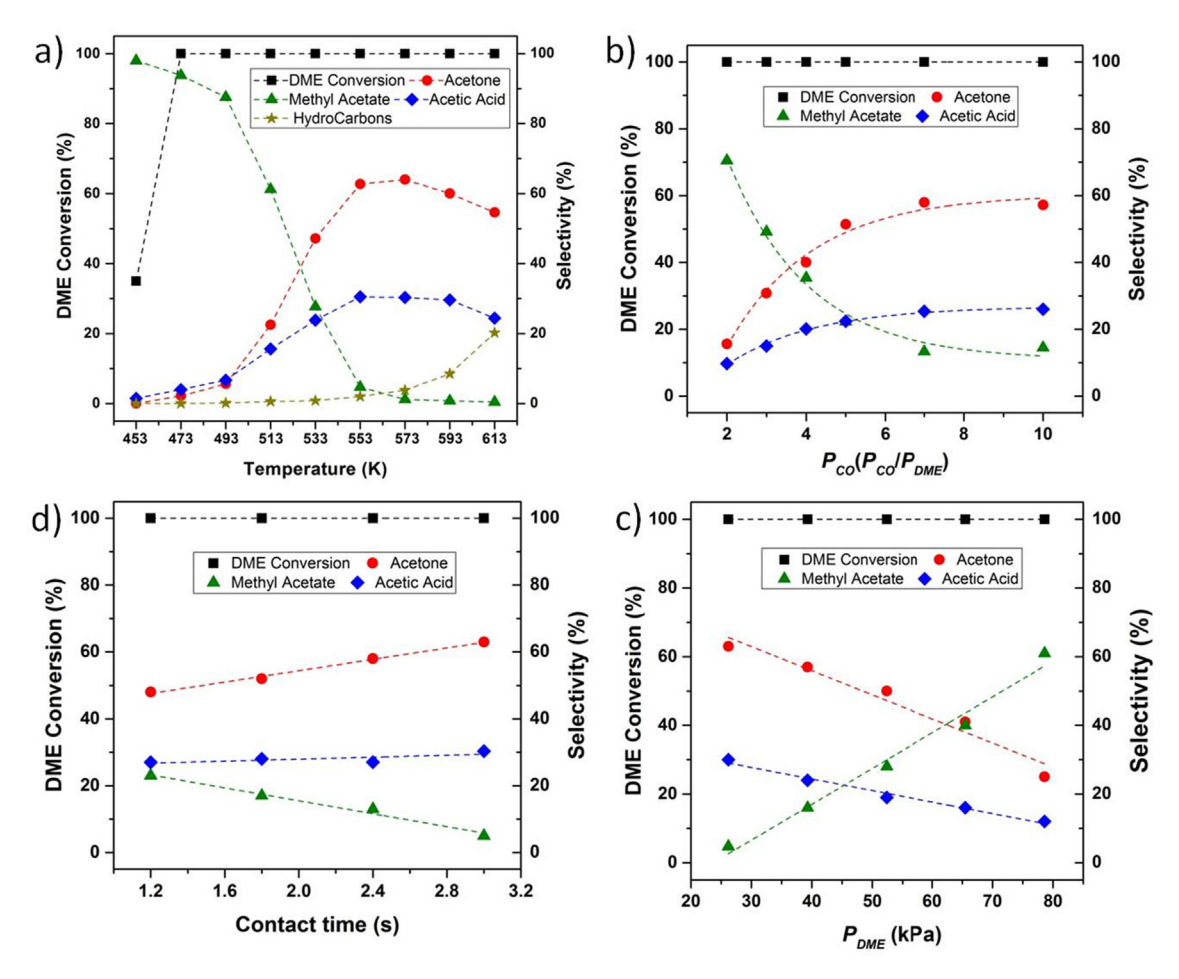


Fig. 2. Effect of (a) temperature (2 MPa,  $P_{DME}$  = 26.2 kPa,  $P_{CO}$  = 420 kPa, total GHSV = 1200 h<sup>-1</sup>), (b)  $P_{CO}$  (553 K, 2 MPa,  $P_{DME}$  = 26.2 kPa, total GHSV = 1200 h<sup>-1</sup>), and (d) contact time (553 K, 2 MPa,  $P_{DME}$  = 26.2 kPa,  $P_{CO}$  = 420 kPa) on DME conversion and acetone selectivity over Py-H-MOR. In all experiments, Ar was used as balancing gas.

## 3.2. Promotion of carbonylation to ketonization

The effect of CO on the ketonization was also examined, as CO is a key reaction component and no relevant study has been reported so far. Therefore, two experiments were performed over Py-H-MOR in the presence and absence of CO to evaluate the contribution of

CO to the ketonization of methyl acetate. The results were also compared with those obtained during the reaction of DME with CO (Fig. 3a).

During the ketonization of methyl acetate in the presence of CO, a selectivity of 68% and 32% was observed for acetone and acetic acid, respectively. However, significantly lower selectivities were

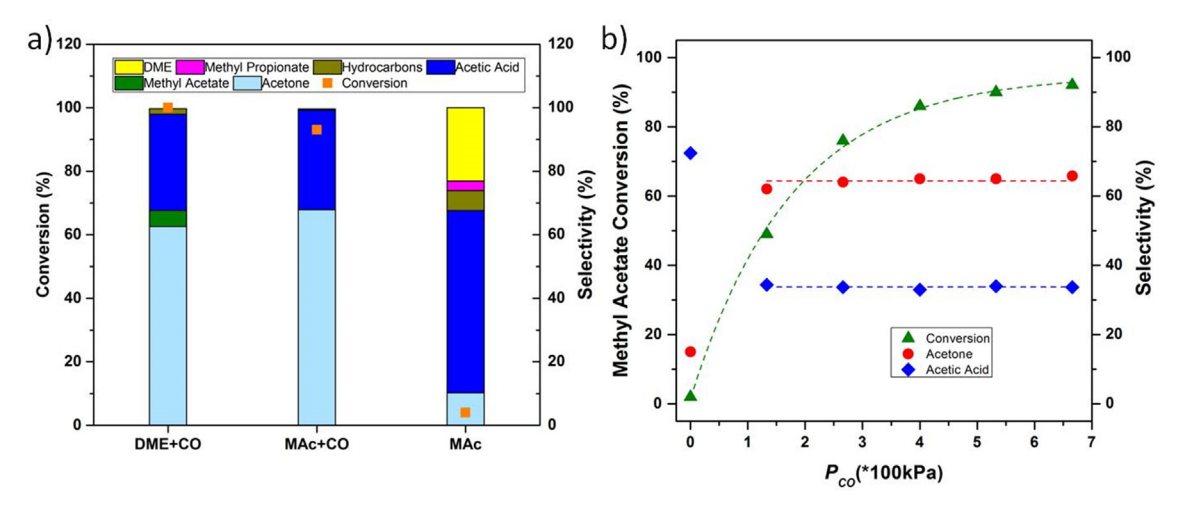


**Fig. 3.** (a) Ketonization of methyl acetate in CO or Ar atmosphere over Py-H-MOR. The orange square indicates the conversion of DME and methyl acetate (MAc) from left to right. Conditions for DME + CO: 553 K, 2 MPa,  $P_{DME}$  = 26.2 kPa,  $P_{CO}$  = 420 kPa, total GHSV = 1200 h<sup>-1</sup>; MAc + CO: 553 K, 2 MPa,  $P_{CO}$  = 666.7 kPa,  $P_{methyl-acetate}$  = 53.8 kPa, total GHSV = 1800 h<sup>-1</sup>; and MAc: 553 K, 2 MPa,  $P_{methyl-acetate}$  = 53.8 kPa, total GHSV = 1800 h<sup>-1</sup>. (b) Effect of  $P_{CO}$  on methyl acetate ketonization over Py-H-MOR (553 K, 2 MPa, total GHSV = 1800 h<sup>-1</sup>,  $P_{methyl-acetate}$  = 53.8 kPa). In all experiments, Ar was used as balancing gas. (For interpretation of the references to colour in this figure legend, the reader is referred to the web version of this article.)

obtained for acetone (10%) and acetic acid (57%) in Ar atmosphere, while the formation of DME (23%), C<sub>4</sub> hydrocarbon (6%), and methyl propionate (4%) was also observed. Based on these results, the product distribution obtained from the reaction of methyl acetate with CO was similar to that of the reaction between DME and CO, where 63% acetone and 30% acetic acid were formed, indicating that CO can greatly affect the ketonization of methyl acetate for highly selective acetone production. Additionally, significant differences were observed between the conversion of methyl acetate (93% in MAc + CO, 4% in MAc) and the selectivity of acetone (68% in MAc + CO, 10% in MAc) during the CO-mediated reaction. Therefore, the effect of  $P_{CO}$  on the ketonization of methyl acetate was also studied. As shown in Fig. 3b, the increase in  $P_{CO}$  values only increased the conversion of methyl acetate, whereas the selectivity of acetone and acetic acid were maintained at 64% and 34%, respectively, further confirming that the ketonization of methyl acetate was significantly promoted by CO.

The treatment of H-MOR with pyridine is an effective method of adjusting its acidity, as pyridine can selectively block the acids in the 12MR channel without affecting the acids in the 8MR side pocket. Since the carbonylation is catalyzed by the acids in the H-MOR side pocket [48], we assumed that the ketonization of methyl acetate can be promoted by the preceding carbonylation step. Indeed, both the conversion of methyl acetate and the selectivity of acetone over Py-H-MOR were higher than over H-MOR (Fig. 4a). Given also that the ability of CO to promote the ketonization of methyl acetate depends on the zeolite topology, the reaction was performed over alternative zeolites, i.e., H-Beta, H-Y, H-ZSM5, and H-ZSM35, to examine their effect on acetone selectivity. However, all four zeolites afforded a low acetone amount with a selectivity of < 10% along with acetic acid, DME, and hydrocarbons (Fig. 4a), probably due to their weak performance in carbonylation [5]. Their pyridine-treated samples were also prepared and tested for their efficiency toward the CO-mediated ketonization of methyl acetate. However, the product distribution was not improved and the conversion of methyl acetate was even lower than over the untreated samples, because nearly all acids were hindered by pyridine (Fig. 4a), indicating that pyridine acts as an acidity modifier rather than a selectivity modifier and does not catalyze the formation of acetone.

To study the evolution of product distribution along the Py-H-MOR, the effect of contact time to the conversion of methyl acetate and the selectivity of acetone were also examined. Upon initial contact of methyl acetate with Py-H-MOR, the selectivity of acetone started to increase, while that of acetic acid gradually decreased, reaching steady  $\sim 65\%$  and  $\sim 35\%$ , respectively. These results confirmed that acetone was obtained from the CO-mediated ketonization of the methyl acetate, while only part of acetic acid contributed to acetone formation at the initial contact with zeolite

Considering that the carbonylation of DME and the subsequent ketonization reaction were catalyzed by the acids in the 8MR side pocket of the catalyst, as proved by the significant difference in acetone selectivity over Py-H-MOR and H-MOR and the Comediated ketonization of methyl acetate, NaH-MOR was used to quantitatively study the role of the acids [48,49]. To that end, six NaH-MOR samples with different Na<sup>+</sup> content were prepared and their IR spectra were recorded. Increasing the Na<sup>+</sup> content in the NaH-MOR samples resulted in a decrease in the IR peaks at 3609 and 3590 cm<sup>-1</sup>, because the proton in the Si–OH–Al moiety in the 12MR main channel and 8MR side pocket of the catalyst was exchanged with Na<sup>+</sup> (Fig. S5).

The IR spectra were further used to determine the quantity of acids following an already reported process [50], and the acetone formation rate was examined as a function of the number of acids in the NaH-MOR samples with varying  $Na^+$  content. Moreover, all samples (n = 6) were treated with pyridine before the experiment, so that only the acids in the 8MR side pocket would be available for the reaction. As shown in Fig. 5a, sample 1# showed poor reactivity due to almost complete ion exchange of its acids. For samples 2#–6#, the acetone formation rate increased with increasing number of acids in the side pocket, and their correlation showed good linearity ( $R^2 = 0.995$ ), indicating that the reaction was catalyzed by the acids in the 8MR side pocket.

The acetone formation rate was also measured using six untreated NaH-MOR samples with the same Na<sup>+</sup> concentrations as before, where the acids were active in both the 8MR side pocket and the 12MR channel of the catalyst (Fig. 5b). Although acetone was formed, the formation rate was much lower than that obtained over the corresponding Py-treated samples due to the active acids

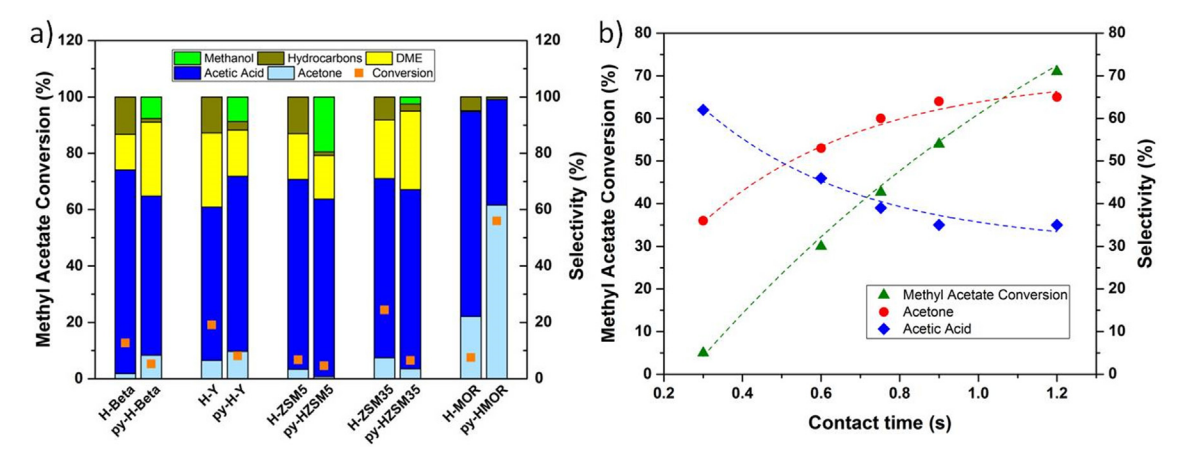


**Fig. 4.** (a) Effect of zeolite topology on the CO-mediated ketonization of methyl acetate (553 K, 1 MPa, total GHSV =  $1800 \, h^{-1}$ ,  $P_{methyl-acetate} = 53.8 \, kPa$ ,  $P_{CO} = 425.5 \, kPa$ , balanced by Ar). (b) Conversion of methyl acetate and selectivity of acetone and acetic acid at different contact times over Py-H-MOR (553 K, 1 MPa,  $P_{methyl-acetate} = 53.8 \, kPa$ ,  $P_{CO} = 333.3 \, kPa$ , balanced by Ar).

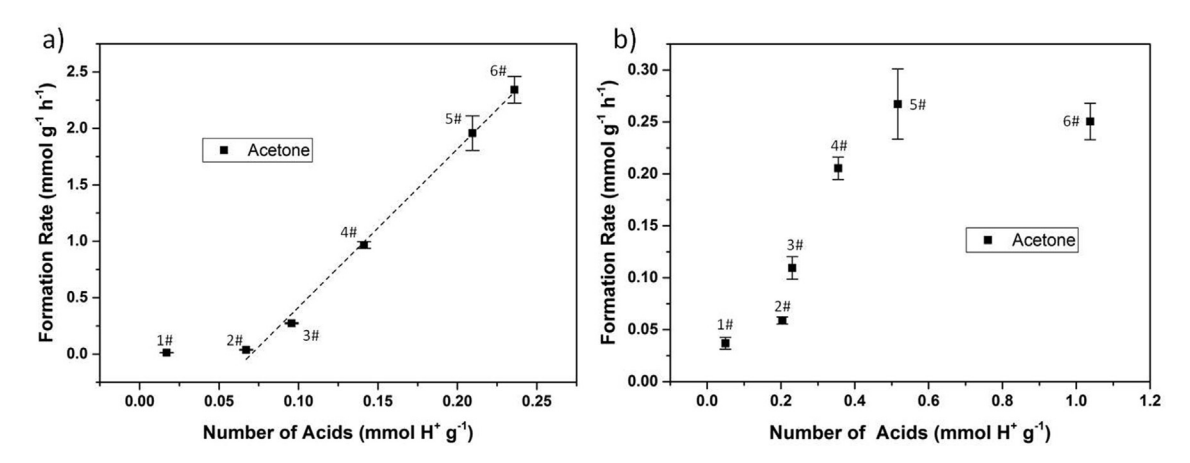


**Fig. 5.** Acetone formation rate per unit mass plotted against the number of acid sites per unit mass of NaH-MOR samples (a) treated and (b) untreated with pyridine at 553 K, 1 MPa, total GHSV = 2250 h<sup>-1</sup>, P<sub>methyl-acetate</sub> = 80 kPa, P<sub>CO</sub> = 333.3 kPa. In all experiments, Ar was used as balancing gas.

of the 12MR channel, which were more likely to consume acetone. Moreover, no specific correlation was observed between the acetone formation rate and the number of acids, confirming that pyridine in the Py-treated samples blocked the acids in the 12MR channel and hindered the acetone consumption.

The ketonization of methyl acetate was also studied under different reaction temperatures (533 and 573 K) to further study the role of CO. The conversion of methyl acetate was higher in the presence of CO, where acetic acid and acetone were mainly formed. In contrast, a significantly different product distribution was observed during CO-free ketonization, affording acetic acid and DME as the main products (Fig. 6a). Other H-zeolites such as H-ZSM5, H-ZSM35, H-Y and H-Beta were also tested for the CO-free ketonization of methyl acetate (Fig. 6b), but afforded a low acetone selectivity (<10%) and high content of acetic acid and DME. The incapability of acetone generation could be caused by the dissociation of methyl acetate over H-zeolites. Studies on the reaction of methyl acetate over H-ZSM5 have revealed that methyl acetate could first alkylate the zeolite (Eq. (4)) [51,52]. In our study, interaction of methyl acetate with the alkyl species on the zeolite then led to the formation of DME (Eq. (5)). In addition, the MTH reaction consumed DME, thus providing water that could hydrolyze the acetyl species (Eq. (6)) and recover the zeolite in its initial form.

$$CH_3COOCH_3 + H$$
-zeolite  $\rightarrow CH_3$ -zeolite +  $CH_3COOH$  (4)

$$CH_3COOCH_3 + CH_3-zeolite \rightarrow CH_3OCH_3 + CH_3CO-zeolite$$
 (5)

$$CH_3CO$$
-zeolite +  $H_2O \rightarrow H$ -zeolite +  $CH_3COOH$  (6)

Consequently, the hydrolysis of methyl acetate (Eq. (7)) and MTH reaction were the main reactions of methyl acetate over Hzeolite. The MTH reaction is complicated and is currently not shown.

$$2CH_3COOCH_3 + H_2O \rightarrow CH_3OCH_3 + 2CH_3COOH$$
 (7)

The ratio of the selectivity of acetic acid to the selectivity of DME was determined at 63.4/30 (%) and 57.6/32.7 (%) during the CO-free ketonization of methyl acetate over Py-H-MOR at 533 K and 553 K, respectively (Fig. 6a), which was similar with the ideal value ( $\sim$ 2) in Eq.7. However, the ratio was>2 when the reaction was performed over other zeolites (Fig. 6b), probably because the MTH reaction was more promoted over H-zeolites than over Py-H-MOR.

Nevertheless, the acetic acid content was particularly high, leading to low methyl acetate conversion, especially over Py-H-MOR. This was attributed to the reversibility of Eq. (7), as the esterification of acetic acid and DME to methyl acetate has a lower acti-

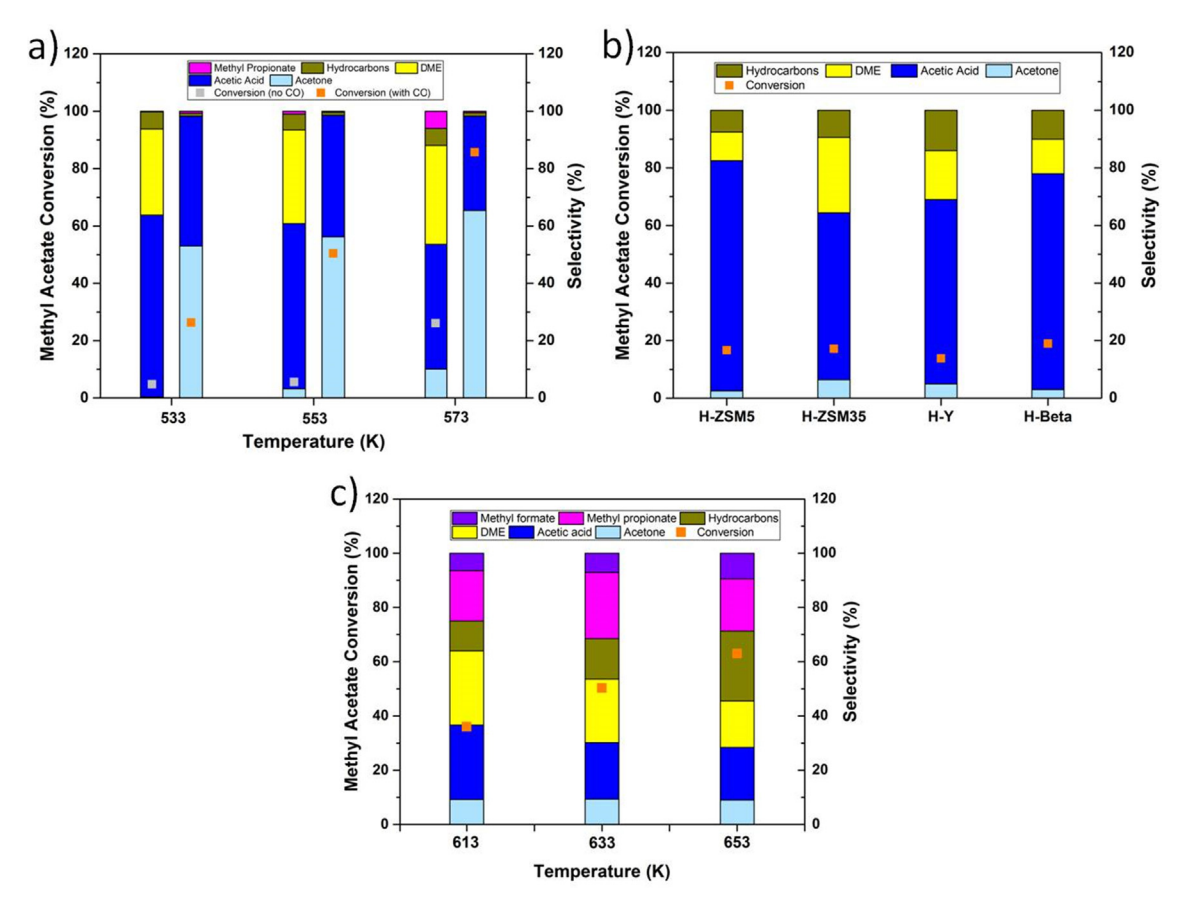


**Fig. 6.** (a) Ketonization of methyl acetate over Py-H-MOR at different temperatures (1 MPa, total GHSV = 1410 h<sup>-1</sup>,  $P_{methyl-acetate}$  = 53.8 kPa,  $P_{CO}$  (if added) = 425.5 kPa). (b) Ketonization of methyl acetate over different H-zeolites (553 K, 1 MPa, total GHSV = 1410 h<sup>-1</sup>,  $P_{methyl-acetate}$  = 53.8 kPa). (c) Ketonization of methyl acetate over Py-H-MOR at 633 K, 1 MPa, total GHSV = 1410 h<sup>-1</sup>, and  $P_{methyl-acetate}$  = 53.8 kPa. In all experiments, Ar was used as balancing gas.

vation energy than the ketonization of acetic acid [53]. Here, we studied the reaction of acetic anhydride and DME to confirm that esterification is easier than ketonization. As shown in Fig. S6, acetone could be produced by the ketonization of acetic anhydride, but the addition of DME increased the formation rate of methyl acetate ( $\sim$ 22  $\times$  10<sup>-4</sup> mol g<sup>-1</sup>h<sup>-1</sup>) by about 7.3 times compared to that of acetone ( $\sim 3 \times 10^{-4} \text{ mol g}^{-1} \text{h}^{-1}$ ). These results could explain the particularly low acetone selectivity and methyl acetate conversion observed in our study during ketonization without CO. Since several zeolite-catalyzed ketonization reactions have been performed at temperatures above 573 K [27,28,54-56], we also examined this temperature (>573 K). A higher temperature (i.e., 633 K) was also applied to stimulate the ketonization of acetic acid, but the selectivity of acetone remained very low (<10%), although the conversion of methyl acetate was significantly improved (Fig. 6c), indicating that the ketonization over Py-H-MOR was not favored under these conditions.

In contrast, a great improvement in acetone selectivity was observed after the CO addition. More specifically, the conversion of methyl acetate and the selectivity of acetone were higher than those observed in the CO-free reaction (Fig. 6a) due to carbonylation. As already mentioned, the ketonization of methyl acetate over Py-H-MOR occurred at the active acids sites of the catalyst's 8MR side pocket, which can also promote carbonylation. Thus, the methyl acetate-derived methoxy species could be then converted to acetyl species [8], as confirmed by the absence of DME in the product mixture, which are important for the subsequent zeolite-catalyzed ketonization [27] and can significantly improve the acetone selectivity. Moreover, the alkylation reaction (Eq. (4)) and the subsequent formation of DME (Eq. (5)) and esterification of acetic

acid with DME (reversed Eq. (7)) were suppressed by carbonylation, resulting in a significantly improved CO-mediated conversion of methyl acetate.

The methoxy and acetyl species of methyl acetate over H-MOR were studied by *in situ* diffuse reflectance IR Fourier transform (DRIFT) spectrometry. It should be noted that we did not use Py-H-MOR for the observation of methoxy species, because the C-H stretching peak of the methyl acetate-derived methoxy species would be covered from that of pyridine. New peaks were detected at 2856, 2960, and 2980 cm<sup>-1</sup> after the adsorption of methyl acetate over H-MOR at 473 K (line 2, Fig. 7a). The peaks at 2960 and 2856 cm<sup>-1</sup> could be assigned to the anti-symmetric and symmetric C-H stretching of the external CH<sub>3</sub>-O-Si species, respectively, while the peak at 2980 cm<sup>-1</sup> was assigned to the C-H stretching of the internal CH<sub>3</sub>-O-Al species [57]. These new peaks indicated that zeolite was successfully alkylated by methyl acetate, which was also consistent with Eq. (4).

The DRIFT spectra could also confirm the formation of acetic acid. Compared to the IR spectrum of Py-H-MOR (line 3, Fig. 7b), the peak intensities at 1710, 1725, and 1745 cm<sup>-1</sup> increased after the adsorption of methyl acetate. The peak at 1725 cm<sup>-1</sup> was assigned to surface-adsorbed acetic acid [27], whereas the peaks at 1710 and 1745 cm<sup>-1</sup> corresponded to acetyl species [8,27], indicating that methyl acetate serves simultaneously as an alkylation and an acylation agent to MOR. The formation of new acetyl species by the addition of CO *via* the carbonylation of the methoxy species, especially those located in the 8MR side pocket, was also observed by *in situ* DRIFT measurements. After the adsorption of methyl acetate over Py-H-MOR (line 4, Fig. 7b), the IR chamber was filled with 2.5 MPa CO. The enhancement of the peak at

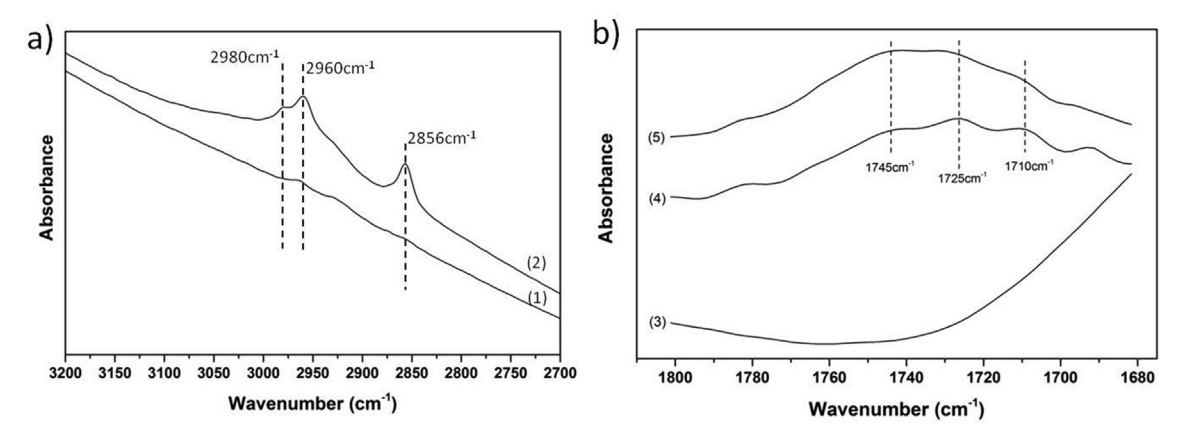


**Fig. 7.** In situ DRIFT study of the methoxy and acetyl species. Spectra of (a) (1) H-MOR, (2) H-MOR flushed by N<sub>2</sub> at 473 K after the adsorption of methyl acetate, (b) The difference spectra of (3) Py-H-MOR at 523 K, (4) Py-H-MOR flushed by N<sub>2</sub> at 523 K after the adsorption of methyl acetate, and (5) Py-H-MOR after the introduction of 2.5 MPa CO to (4) for 3 min at 523 K, to the spectra of Py-H-MOR at 523 K.

 $1745~\text{cm}^{-1}$  (line 5, Fig. 7b) indicated the generation of new acetyl species.

The role of carbonylation in the ketonization of methyl acetate could be further studied by TPD analysis, even two reactions were performed at different temperature.. The ion current of acetone (*m*/ e = 58) was measured by MS to evaluate the formation of acetone with increasing temperature. According to Fig. 8, acetone was hardly generated as the temperature increased during the COuntreated desorption (black line). Although the importance of acetyl species in the ketonization over zeolite has been previously reported [27] and methyl acetate can sufficiently provide acetyl species, the methoxy species formed in our study seem to hinder the CO-free ketonization. In contrast, acetone production was detected at 500 K upon treatment with static 1 MPa CO at 473 K (Fig. 8, red line), as new acetyl species could be generated. These results were consistent with our previous findings in the current study and highlighted the importance of carbonylation to the ketonization of methyl acetate and the production of acetone with high selectivity.

The participation and the final location of CO in acetone formation was further studied isotopically by GC-MS. The main

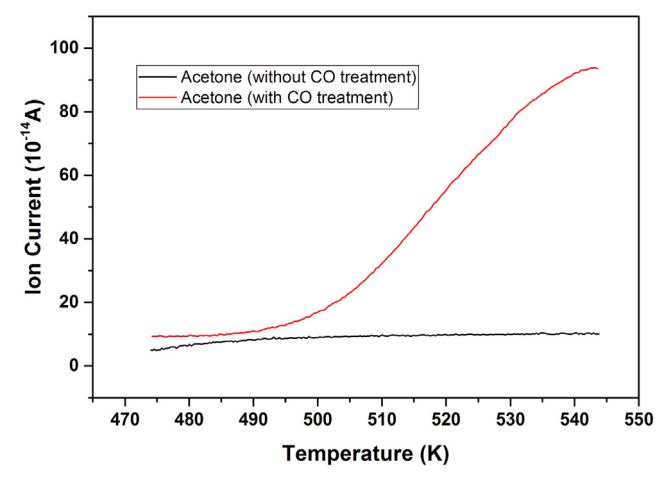


**Fig. 8.** Acetone (m/e = 58) formation during TPD analysis. The acetone signal of the CO-free desorption was recorded after the adsorption of methyl acetate at 473 K (black line). For the CO-mediated experiment (red line), the catalyst was treated after the adsorption of methyl acetate with static 1 MPa CO at 473 K for 1 h, decompressed to ambient pressure, and flushed by Ar, and then the temperature was increased. (For interpretation of the references to colour in this figure legend, the reader is referred to the web version of this article.)

fragments of acetone obtained from the carbonylation of DME with  $^{13}$ CO were at m/e = 59 and 44, while those of CO<sub>2</sub> were found at m/ee = 45 and 29. In contrast, the corresponding peaks using commercial CO were detected at m/e = 58 and 43 for acetone, and at m/ee = 44 and 28 for  $CO_2$  (Fig. 9). The mass difference suggested that CO contributed to the carbonyl (C=O) group of acetone ( $CH_3^{13}$ - $COCH_3$ ) and the formation of  $CO_2$  ( $^{13}CO_2$ ). In addition, the reaction of methyl acetate and <sup>13</sup>CO afforded acetone in a mixture of CH<sub>3</sub><sup>12</sup>- $COCH_3$  and  $CH_3^{13}COCH_3$  with two fragments at m/e = 58/59 and 43/44, while a fragment at m/e = 44/45 was detected for CO<sub>2</sub> corresponding to a mixture of <sup>12</sup>CO<sub>2</sub> and <sup>13</sup>CO<sub>2</sub>. The results demonstrated that CO also participated in the generation of acetone through carbonylation and showed that the carbonyl group migrated over the zeolite during ketonization. Moreover, the isotopic studies suggested that both the carbonyl carbon of acetone and CO2 originated from the carbonyl carbon atom of the acetyl group. The corresponding reactions could be expressed by Eqs. (8), Eqs. (9) and (10), which show the DME carbonylation to methyl acetate, CO-mediated ketonization of methyl acetate and the overall coupling reaction.

$$CH_3OCH_3 + CO \rightarrow CH_3COOCH_3$$
 (8)

$$CH_3COOCH_3 + CO \rightarrow CH_3COCH_3 + CO_2$$
 (9)

$$CH_3OCH_3 \ + \ 2CO \ \rightarrow \ CH_3COOCH_3 \ + \ CO_2 \eqno(10)$$

## 3.3. Ketonization mechanism

Despite the importance of acetyl species in the zeolitecatalyzed ketonization, the mechanism of the acetyl species conversion to acetone and CO<sub>2</sub> has not been extensively studied. Considering that the formation of a new C-C bond is involved, we herein suggested that the ketonization reaction involves the formation of a ketene intermediate. The ketene is in equilibrium with acetyl species by leaving an  $\alpha$ -hydrogen [19] at the ketonization temperature. The prediction of the ketene formation by density functional theory calculations and the indirect experimental capture of ketene in DME carbonylation has been reported in a previous study, where the ketene and acetyl species could be distinguished by the formation of CH<sub>3</sub>COOD. The reaction of D<sub>2</sub>O with ketene would also yield  $CH_2DCOOD$  (m/e = 62), which would in turn generate  $CH_3COOD$  (m/e = 61) upon reaction with acetyl species. [35] Therefore, in this study, we used the same strategy to capture and study ketene and further elucidate the ketonization

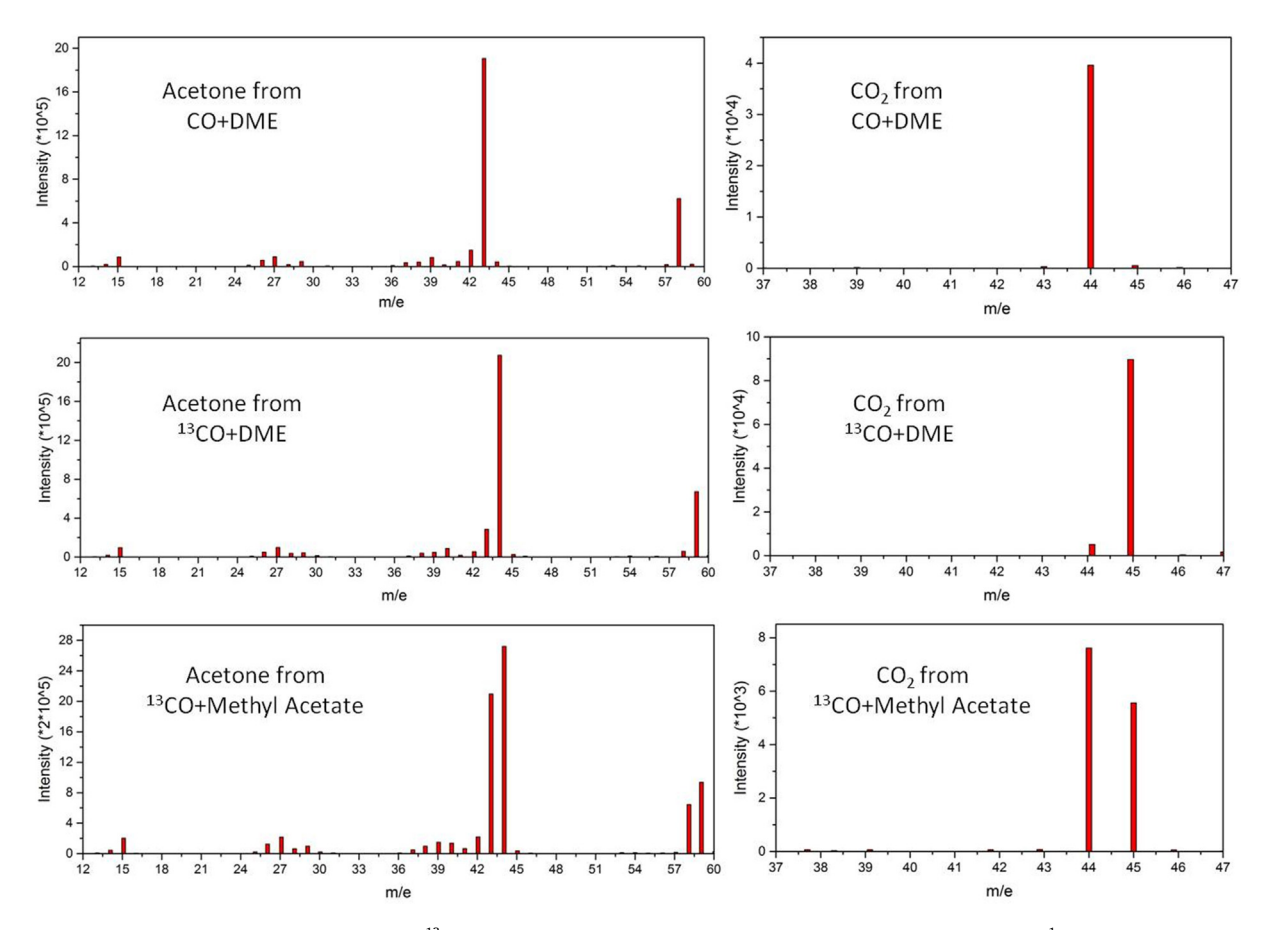


**Fig. 9.** GC-MS spectrum of acetone and CO<sub>2</sub> derived from  $^{13}$ CO. Reaction conditions for CO + DME: 553 K, 1 MPa, total GHSV = 675 h<sup>-1</sup>,  $P_{DME}$  = 27.3 kPa,  $P_{CO}$  = 222.2 kPa;  $^{13}$ CO + DME: 553 K, 1 MPa, total GHSV = 675 h<sup>-1</sup>,  $P_{DME}$  = 27.3 kPa,  $P_{CO}$  = 222.2 kPa,  $P_{He}$  = 222.2 kPa;  $^{13}$ CO + methyl acetate: 553 K, 1 MPa, total GHSV = 840 h<sup>-1</sup>,  $P_{methyl-acetate}$  = 53.8 kPa,  $P_{CO}$  = 142.8 kPa,  $P_{He}$  = 142.8 kPa. All experiments were performed over Py-H-MOR for 1 h and Ar was used as balancing gas.

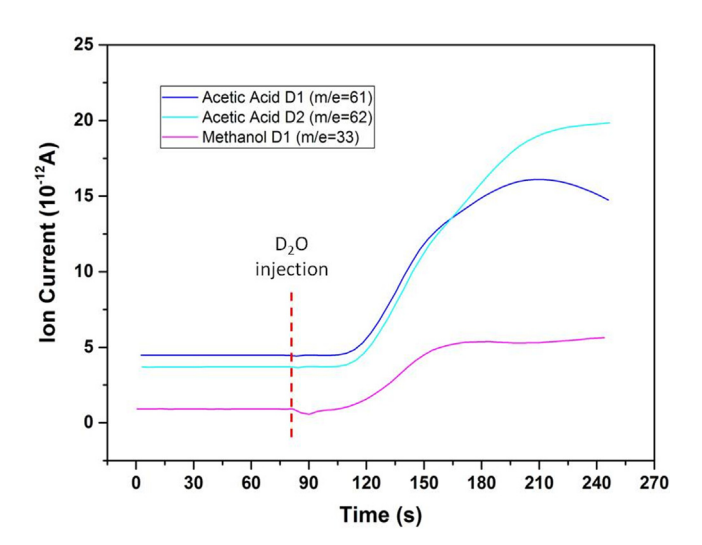


**Fig. 10.** MS spectra of CH<sub>3</sub>OD (m/e = 33), CH<sub>3</sub>COOD (m/e = 61), and CH<sub>2</sub>DCOOD (m/e = 62) after injection of 0.3 mL D<sub>2</sub>O (553 K, 1 MPa,  $P_{DME}$  = 17.2 kPa,  $P_{CO}$  = 444.4 kPa, balanced by Ar, total GHSV = 1350 h<sup>-1</sup> over Py-H-MOR). The  $\times$  axis refers to the time around the D<sub>2</sub>O injection moment.

mechanism. As shown in the MS spectrum (Fig. 10), the pulse injection of 0.3 mL  $D_2O$  during the carbonylation of DME to acetone rapidly increased the signals at m/e = 62 and 61, indicating the

existence of both ketene and acetyl species.  $CH_3OD$  was also formed by  $D_2O$  hydrolysis of the methoxy species. It should be noted that  $D_2O$  was injected 100 min after the start of the carbonylation reaction to ensure that acetone was formed from DME carbonylation.

Furthermore, the presence of ketene could be confirmed by the detection of two types of pyrones in the spent Py-H-MOR catalyst. 3,5-Dimethyl phenol, resulting from the aldol condensation of acetone [58,59], and pyrones were the main identified coke species (Fig. 11). Dehydroacetic acid and 2,6-dimethyl-4-pyrone were also found in the spent catalyst. In addition, a diketene could be easily formed by the condensation of two ketenes, and could be further dipolymerized to dehydroacetic acid or 3-carboxy-2,6-dimethyl-4-pyrone, which can subsequently afford 2,6-dimethyl-4-pyrone *via* decarboxylation [60] (Scheme 1).

To confirm that these two pyrones derived from the ketene intermediate, their GC–MS spectra obtained using <sup>12</sup>CO and <sup>13</sup>CO were compared (Fig. 12). The molecular weight of dehydroacetic acid obtained by the reaction of DME with <sup>13</sup>CO and the reaction of methyl acetate with <sup>12</sup>CO was 172 and 168, respectively. These mass values corresponded to the total mass of ketenes needed to polymerize and their difference indicated the number of ketenes involved in the reaction, suggesting that dehydroacetic acid was formed *via* ketene polymerization. The molecular weight of 2,6-dimethyl-4-pyrone obtained from the same reactions was 127 and 124, respectively. Due to the loss of a carboxyl group as CO<sub>2</sub>, the mass difference was 3, which could however prove the formation of 2,6-dimethyl-4-pyrone from ketene.

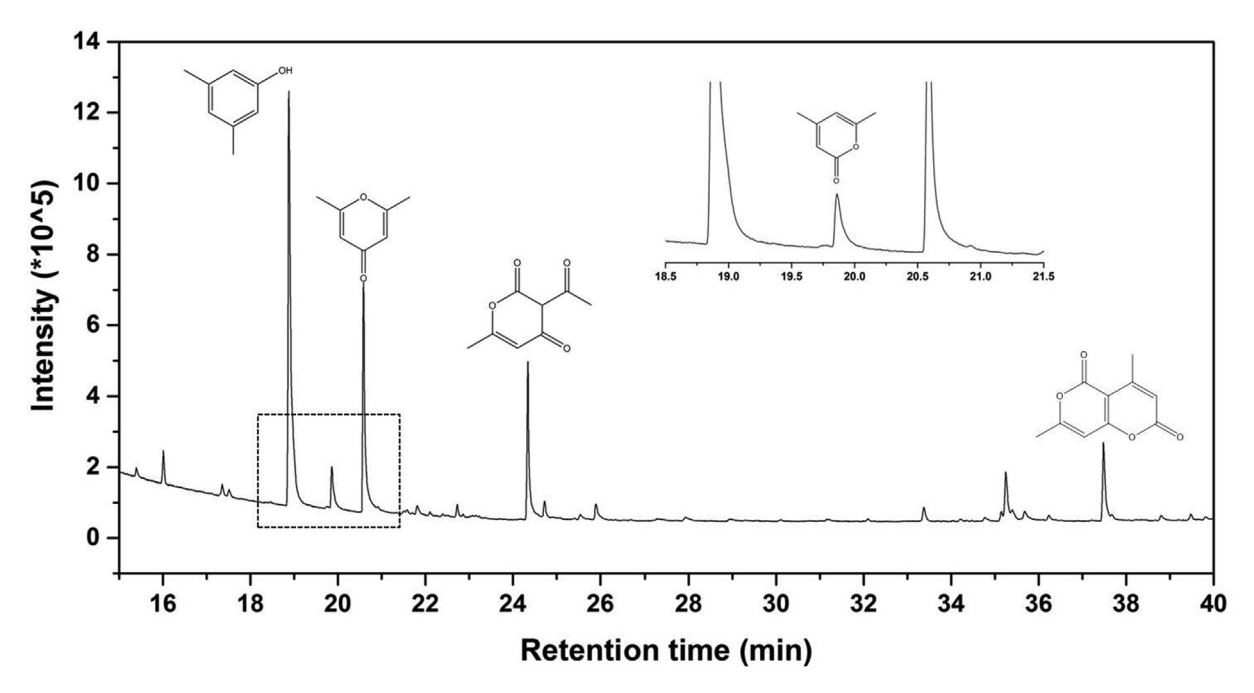
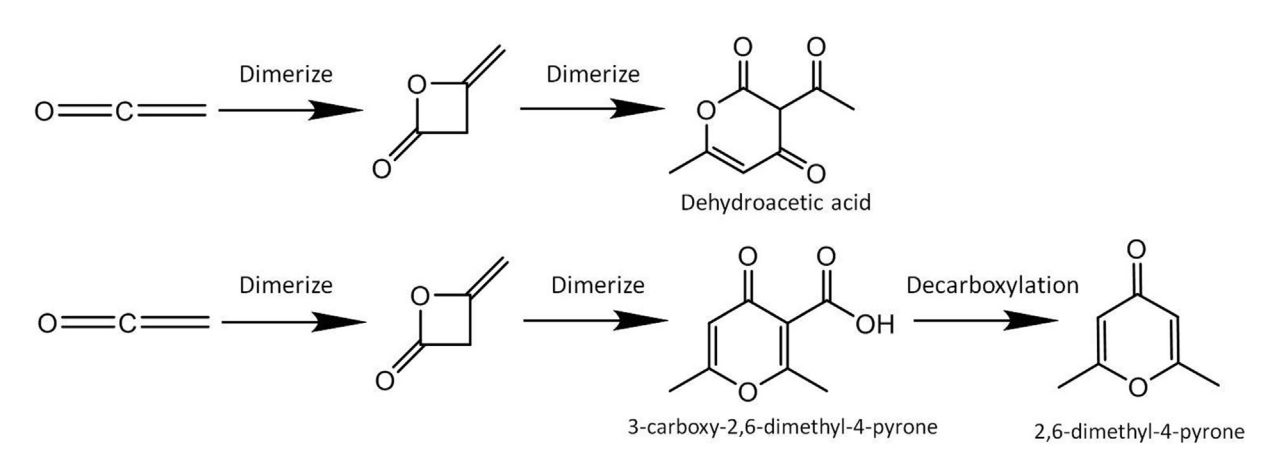


Fig. 11. GC-MS spectrum of the coke species deposited in the spent Py-H-MOR catalyst.



Scheme 1. Condensation of ketene and dimerization of diketene to dehydroacetic acid and 2,6-dimethyl-4-pyrone [59].

Moreover, the molecular weight of dehydroacetic acid obtained from the methyl acetate +  $^{13}$ CO reaction varied from 168 to 172 (Fig. 13a), suggesting that the amount of  $^{13}$ C derived from  $^{13}$ CO in dehydroacetic acid varied from 0 to 4 due to the different possible combinations of CH<sub>2</sub>= $^{12}$ C=O and CH<sub>2</sub>= $^{13}$ C=O for polymerization to dehydroacetic acid. The molecular weight distribution of dehydroacetic acid was also converted to the corresponding distribution of the  $^{13}$ C amount (Fig. 13c), which could be fitted into the following binominal distribution.

$$\begin{split} B\ (X=k,n=4,P=47.5\%) &= \binom{k}{4} P^k (1-P)^{4-k}, where \\ k=0-4\ and\ \binom{k}{4} &= \frac{4!}{k!(4-k)!} \end{split} \ \ (11) \end{split}$$

The GC–MS spectrum of 2,6-dimethyl-4-pyrone obtained by the reaction of methyl acetate with <sup>13</sup>CO (Fig. 13b) revealed that its molecular weight varied from 124 to 127, indicating that the combination of ketene is also possible in this reaction. The molecular

weight distribution was further converted to the corresponding probability distribution. However, due to decarboxylation for the formation of 2,6-dimethyl-4-pyrone, the binominal distribution (Eq. (11)) could not be directly used. Thus, only the possibilities for k = 0-3 were considered for the calculation (Eq. (12)) using B'(X = k, n = 4, P = 44%) based on B(X = k, n = 4, P = 44%) (Fig. 13d).

$$B^{'}(X=k,n=4,P=44\%) = \frac{\binom{k}{4}P^k(1-P)^{4-k}}{\sum_{i=0}^{3}\binom{i}{4}P^i(1-P)^{4-i}}, \text{where } k=0-3$$
 (12)

Parameter P is the probability of  $CH_2$ = $^{13}C$ =O participating in the ketene polymerization reaction. Considering also the natural  $^{13}C$  abundance, the ideal probability should be 50.5% because the reaction of methyl acetate with  $^{13}CO$  provides one  $CH_2$ = $^{13}C$ =O ketene via carbonylation and one  $CH_2$ = $^{12}C$ =O ketene from the acetyl group of methyl acetate.  $CH_2$ = $^{12}C$ =O and  $CH_2$ = $^{13}C$ =O can be distinguished by the isotope effect.  $CH_2$ = $^{13}C$ =O is less likely to participate in the reaction because more energy is required to break a

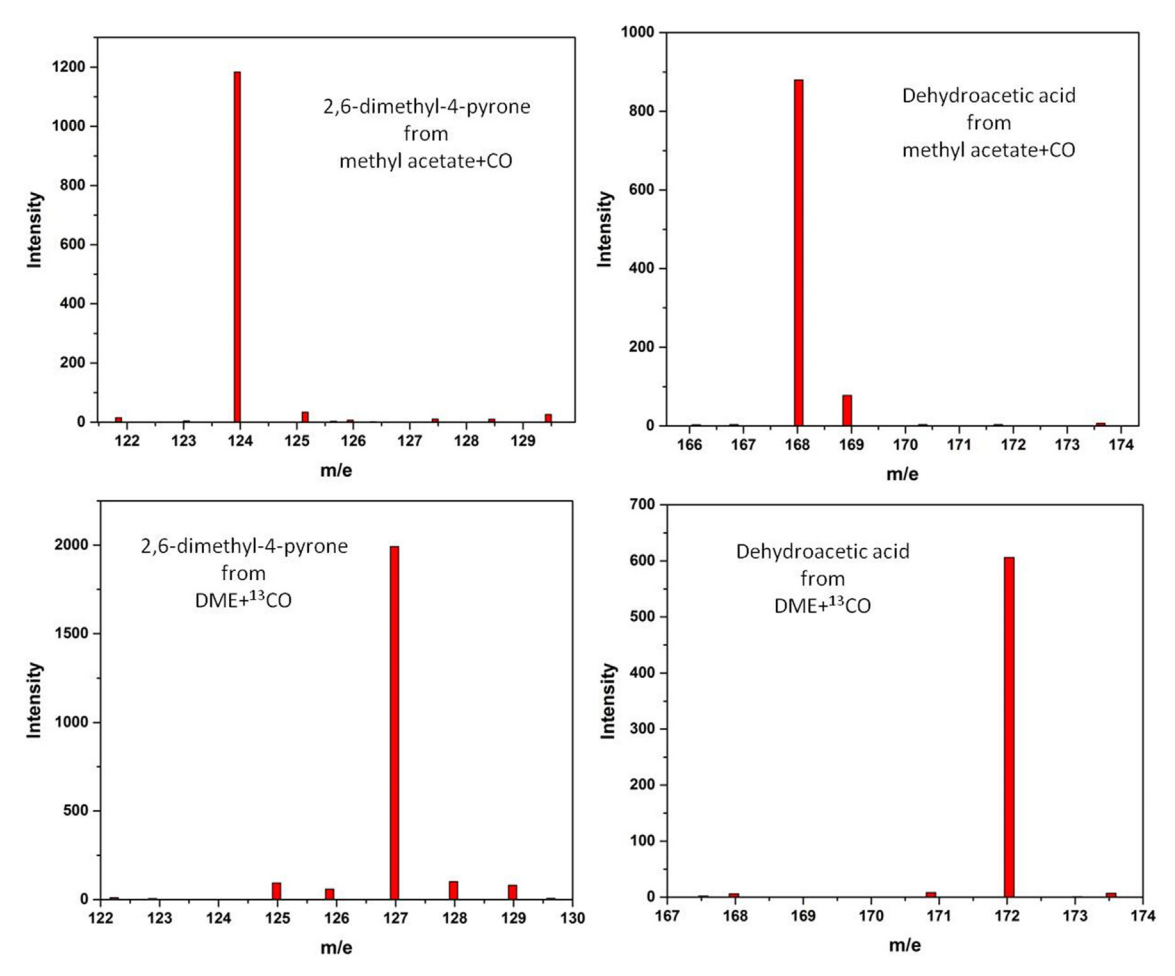


**Fig. 12.** Molecular weight of dehydroacetic acid and 2,6-dimethyl-4-pyrone obtained from the reactions of DME +  $^{13}$ CO (553 K, 1 MPa, total GHSV = 675 h<sup>-1</sup>,  $P_{DME}$  = 27.3 kPa,  $P_{CO}$  = 222.2 kPa,  $P_{He}$  = 222.2 kPa,  $P_{He}$  = 222.2 kPa, balanced by Ar, Py-H-MOR, 1 h) and methyl acetate +  $^{12}$ CO (553 K, 1 MPa, total GHSV = 1410 h<sup>-1</sup>,  $P_{methyl-acetate}$  = 53.8 kPa,  $P_{CO}$  = 425.5 kPa, balanced by Ar, Py-H-MOR).

bond directly linked to an isotopic atom [61]. Namely,  $^{12}C^{-12}C$  can break more easily than  $^{12}C^{-13}C$ , leading to P < 50.5% for  $CH_2$ = $^{13}C$ =O.

As already shown in Fig. 9, the imbalanced intensity of m/e = 43 and 44 in acetone and that of m/e = 44 and 45 in CO<sub>2</sub> obtained from the methyl acetate +  $^{13}$ CO reaction indicated that ketonization was affected by the kinetic isotope effect (KIE). If CH<sub>2</sub>= $^{13}$ C=O and CH<sub>2</sub>= $^{12}$ C=O contributed equally to the reaction, the probability for acetone should also be equally distributed to acetone and CO<sub>2</sub> considering the natural  $^{13}$ C abundance. However, acetone was more likely to be isotopic labeled than CO<sub>2</sub> and their respective P values were 56.5% and 42.2%, which allowed the suggestion of a reaction mechanism for ketonization over zeolite.

The mechanism of the carbonylation-assisted ketonization of methyl acetate is shown in Scheme 2. The formation of methyl acetate by DME carbonylation is not shown, because it has already been studied [8]. Methyl acetate first alkylates the zeolite, thus generating methoxy species and acetic acid. Acetyl species are then formed by the acylation of acetic acid and the carbonylation of methoxy species. The acetyl species can be subsequently transformed to ketene through an  $\alpha$ -hydrogen elimination. The  $C_\beta$  (carbon at  $\beta$ -position relative to oxygen) and  $C_\alpha$  (carbon at  $\alpha$ -position relative to oxygen) atoms of  $CH_2$ =12C=O are negatively and position

tively charged, respectively, thus allowing the nucleophilic addition of  $C_{\beta}$  to a positively charged atom [62]. Hence, the nucleophilic addition of ketene to the positively charged acetyl species yields an acetoacetyl intermediate, which affords acetoacetic acid upon reaction with water and decomposes into acetone and  $CO_2$  *via* decarboxylation. Acetone is finally produced from one of the two acetyl species, whereas the other acetyl species turns into ketene, thus contributing to the alkyl group of acetone and the formation of  $CO_2$ .

When  $^{13}\text{CO}$  was used for the methyl acetate ketonization, compared with  $\text{CH}_2=^{12}\text{C}=0$ , it is more difficult for  $\text{CH}_2=^{13}\text{C}=0$  to participate in the nucleophilic addition to acetyl species due to KIE. For  $\text{CH}_2=^{13}\text{C}=0$ , it converts back into acetyl species and attacked by  $\text{CH}_2=^{12}\text{C}=0$ , which eventually leads to  $^{13}\text{C}$  accumulation in the acetyl species, resulting in acetone, and  $\text{CO}_2$  with  $^{13}\text{C}$  content above and below 50.5%, respectively. The primary KIE reported in the literature for  $^{12}\text{C}/^{13}\text{C}$  is about 1.04 [63–65], and the possibility shift in acetone derived from the methyl acetate +  $^{13}\text{CO}$  reaction is 56.2%/50.5%=1.113. Here, this can be caused by the double breaking of the C=C ketene bond during the formation of acetoacetyl species *via* the nucleophilic addition of ketene to acetyl species, and the decarboxylation of acetoacetic acid with a possibility shift of  $1.04^2=1.082$ , a value very close to 1.113.

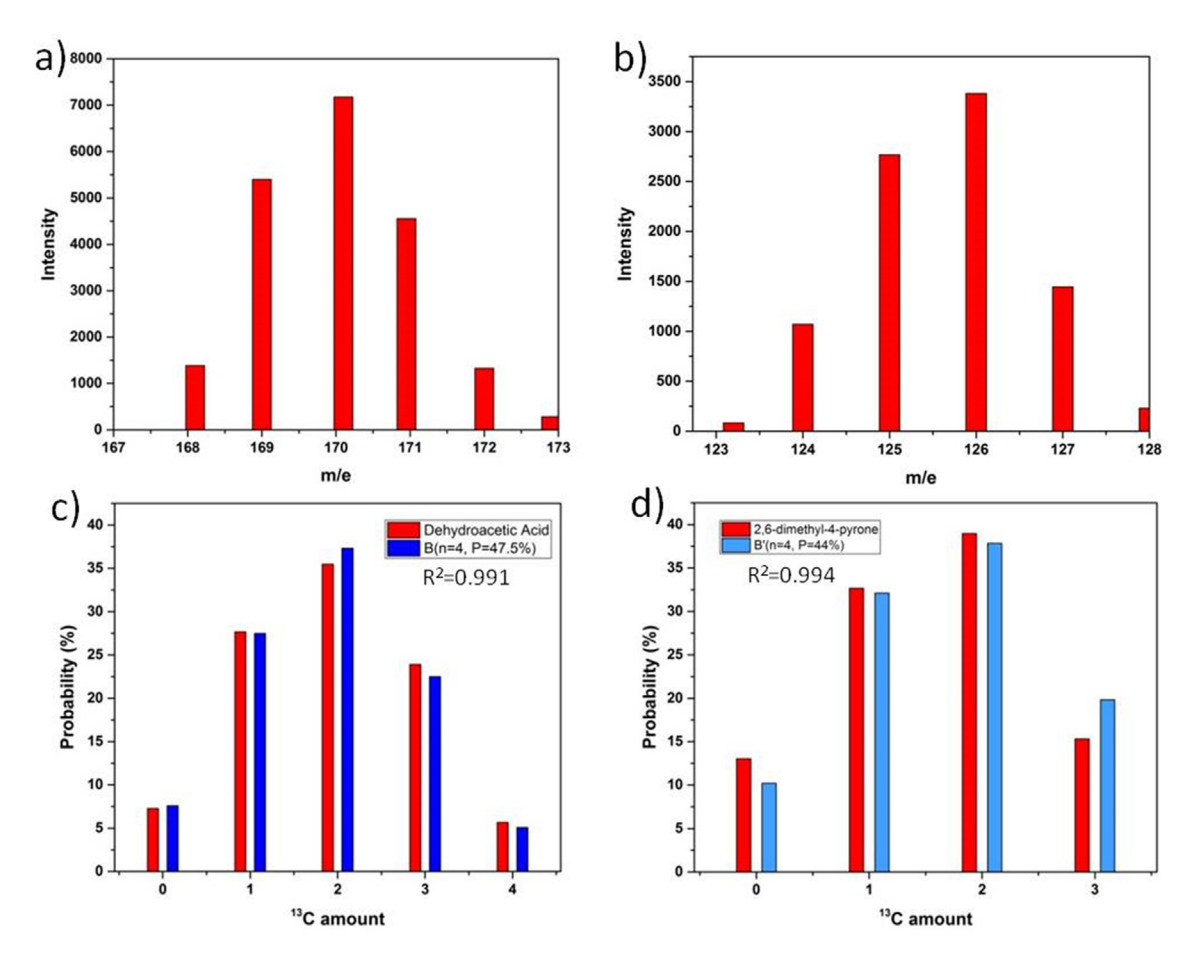
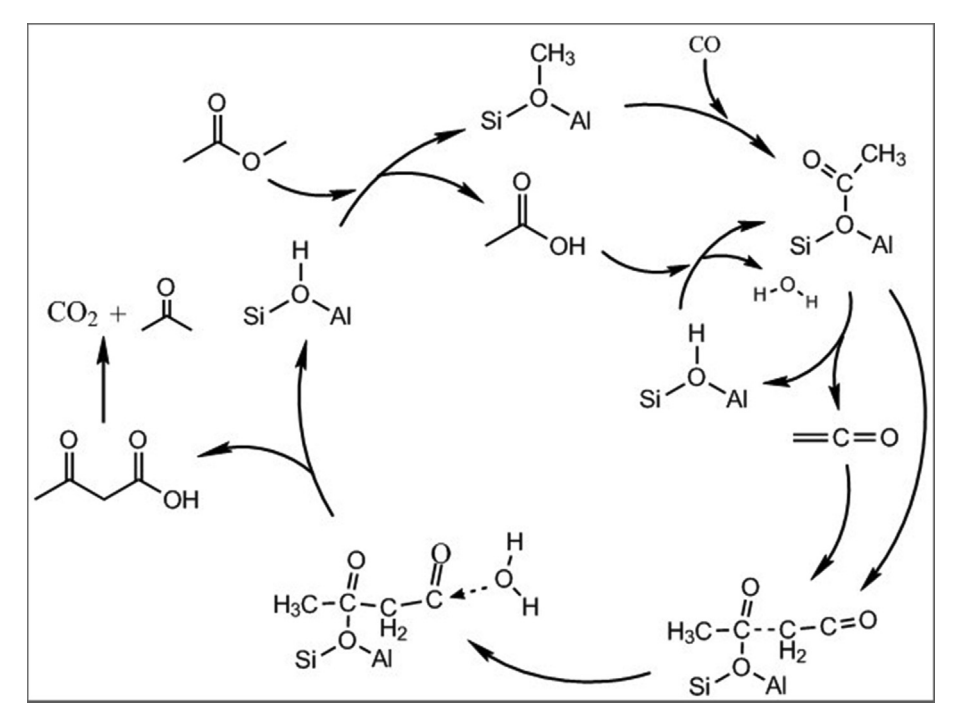


**Fig. 13.** GC–MS spectra of (a) dehydroacetic acid and (b) 2,6-dimethyl-4-pyrone obtained from the methyl acetate  $^{+13}$ CO reaction (553 K, 1 MPa, total GHSV = 840 h<sup>-1</sup>,  $P_{methyl-acetate}$  = 53.8 kPa,  $P_{CO}$  = 142.8 kPa,  $P_{He}$  = 142.8 kPa, Py-H-MOR, 1 h, balanced by Ar). (c) Conversion of molecular weight distribution to probability of  $^{13}$ C amount distribution fitted by Eq. (11). (d) Conversion of molecular weight distribution to probability of  $^{13}$ C amount distribution fitted by Eq. (12).



**Scheme 2.** Proposed reaction mechanism of methyl acetate ketonization for acetone formation.

#### 4. Conclusions

A novel acetone production method was developed based on the carbonylation of DME to methyl acetate and its subsequent ketonization to acetone. The reaction cascade was catalyzed by the acid sites in the 8MR side pocket of H-MOR, and the acetone selectivity was significantly enhanced using Py-H-MOR as the catalyst, as side reactions consuming acetone were efficiently suppressed by pyridine. In addition, we found that the carbonylation step is important for promoting the conversion of methyl acetate and improving the acetone selectivity. In situ DRIFT studies showed that methyl acetate served as both an alkylation and acylation agent for H-MOR, and new acetyl species were generated by the carbonylation reaction. The participation of CO in the ketonization of methyl acetate was confirmed by isotopic experiments, while the formation of a ketene intermediate was verified by the formation of CH<sub>2</sub>DCOOD using D<sub>2</sub>O and the presence of 2,6-dimethyl-4pyrone and dehydroacetic acid in the spent catalyst. According to the binominal distribution of <sup>13</sup>C in the two pyrone types obtained by the  $^{13}$ CO-involved ketonization of methyl acetate, CH<sub>2</sub>= $^{13}$ C=0 was less likely to participate in the nucleophilic addition than CH<sub>2</sub>=<sup>12</sup>C=O due to the KIE. A mechanism for the ketonization reaction toward acetone and CO2 was also proposed involving the formation of a ketene intermediate, indicating that the acetyl species contribute to the acyl part of acetone, while ketene is involved in the formation of the acetone alkyl group and CO<sub>2</sub>.

#### **Author Contributions**

All authors have given approval to the final version of the manuscript.

#### **Funding Sources**

We acknowledge the financial support from the National Natural Science Foundation of China (Grant No. 21972141, Grant No.21978285, Grant No. 21,991,090 and Grant No. 21991094,), and the "Transformational Technologies for Clean Energy and Demonstration", Strategic Priority Research Program of the Chinese Academy of Sciences (Grant No. XDA21030100).

#### **Declaration of Competing Interest**

The authors declare that they have no known competing financial interests or personal relationships that could have appeared to influence the work reported in this paper.

## Appendix A. Supplementary material

Supplementary data to this article can be found online at https://doi.org/10.1016/j.jcat.2021.03.006.

### References

- P. Tian, Y. Wei, M. Ye, Z. Liu, Methanol to Olefins (MTO): From Fundamentals to Commercialization, ACS Catal. 5 (2015) 1922–1938.
- [2] Y. Wang, A new horizontal in C1 chemistry: Highly selective conversion of syngas to light olefins by a novel OX-ZEO process, J. Energy Chem. 25 (2016) 169–170.
- [3] J. Sun, G. Yang, Y. Yoneyama, N. Tsubaki, Catalysis Chemistry of Dimethyl Ether Synthesis, ACS Catal. 4 (2014) 3346–3356.
- [4] K. Fujimoto, T. Shikada, K. Omata, H. Tominaga, Vapor phase carbonylation of methanol with solid acid catalysts, Chem. Lett. (1984) 2047–2050.
- [5] P. Cheung, A. Bhan, G.J. Sunley, E. Iglesia, Selective carbonylation of dimethyl ether to methyl acetate catalyzed by acidic zeolites, Angew. Chem. Int. Ed. 45 (2006) 1617–1620.
- [6] S.Y. Park, C.-H. Shin, J.W. Bae, Selective carbonylation of dimethyl ether to methyl acetate on Ferrierite, Catal. Commun. 75 (2016) 28–31.

- [7] H. Zhou, W. Zhu, L. Shi, H. Liu, S. Liu, Y. Ni, Y. Liu, Y. He, S. Xu, L. Li, Z. Liu, In situ DRIFT study of dimethyl ether carbonylation to methyl acetate on Hmordenite, J. Mol. Catal. A: Chem. 417 (2016) 1–9.
- [8] P. Cheung, A. Bhan, G. Sunley, D. Law, E. Iglesia, Site requirements and elementary steps in dimethyl ether carbonylation catalyzed by acidic zeolites, J. Catal. 245 (2007) 110–123.
- [9] M. Boronat, C. Martínez-Sánchez, D. Law, A. Corma, Enzyme-like Specificity in Zeolites: A Unique Site Position in Mordenite for Selective Carbonylation of Methanol and Dimethyl Ether with CO, J. Am. Chem. Soc. 130 (2008) 16316– 16323
- [10] M. Boronat, C. Martinez, A. Corma, Mechanistic differences between methanol and dimethyl ether carbonylation in side pockets and large channels of mordenite, Phys. Chem. Chem. Phys. 13 (2011) 2603–2612.
- [11] T. He, X. Liu, S. Xu, X. Han, X. Pan, G. Hou, X. Bao, Role of 12-Ring Channels of Mordenite in DME Carbonylation Investigated by Solid-State NMR, J. Phys. Chem. C 120 (2016) 22526–22531.
- [12] M.V. Luzgin, M.S. Kazantsev, G.G. Volkova, W. Wang, A.G. Stepanov, Carbonylation of dimethyl ether on solid Rh-promoted Cs-salt of Keggin 12– H<sub>3</sub>PW<sub>12</sub>O<sub>40</sub>: A solid-state NMR study of the reaction mechanism, J. Catal. 277 (2011) 72–79.
- [13] M. Boronat, C. Martinez-Sanchez, D. Law, A. Corma, Enzyme-like Specificity in Zeolites-A Unique Site Positon in MOR for Selective Carbonylation of Methanol and DME with CO, J. Am. Chem. Soc. 130 (2008) 16316–16323.
- [14] S. Wang, W. Guo, L. Zhu, H. Wang, K. Qiu, K. Cen, Methyl Acetate Synthesis from Dimethyl Ether Carbonylation over Mordenite Modified by Cation Exchange, J. Phys. Chem. C 119 (2015) 524–533.
- [15] A.A.C. Reule, N. Semagina, Zinc Hinders Deactivation of Copper-Mordenite: Dimethyl Ether Carbonylation, ACS Catal. 6 (2016) 4972–4975.
- [16] J. Liu, H. Xue, X. Huang, P.-H. Wu, S.-J. Huang, S.-B. Liu, W. Shen, Stability Enhancement of H-Mordenite in Dimethyl Ether Carbonylation to Methyl Acetate by Pre-adsorption of Pyridine, Chin. J. Catal. 31 (2010) 729– 738.
- [17] H. Xue, X. Huang, E. Zhan, M. Ma, W. Shen, Selective dealumination of mordenite for enhancing its stability in dimethyl ether carbonylation, Catal. Commun. 37 (2013) 75–79.
- [18] T.N. Pham, D. Shi, D.E. Resasco, Evaluating strategies for catalytic upgrading of pyrolysis oil in liquid phase, Appl. Catal. B 145 (2014) 10–23.
- [19] T.N. Pham, T. Sooknoi, S.P. Crossley, D.E. Resasco, Ketonization of Carboxylic Acids: Mechanisms, Catalysts, and Implications for Biomass Conversion, ACS Catal. 3 (2013) 2456–2473.
- [20] D.E. Resasco, B. Wang, S. Crossley, Zeolite-catalysed C-C bond forming reactions for biomass conversion to fuels and chemicals, Catal. Sci. Technol. 6 (2016) 2543–2559.
- [21] M. Gliński, G. Zalewski, E. Burno, A. Jerzak, Catalytic ketonization over metal oxide catalysts. XIII. Comparative measurements of activity of oxides of 32 chemical elements in ketonization of propanoic acid, Appl. Catal. A 470 (2014) 278–284.
- [22] M. Glinski, J. Kijenski, A. Jakubowski, Ketones from monocarboxylic acids catalytic ketonization over oxide systems, Appl. Catal. A: GEN 128 (1995) 209– 217
- [23] S. Wang, E. Iglesia, Experimental and theoretical assessment of the mechanism and site requirements for ketonization of carboxylic acids on oxides, J. Catal. 345 (2017) 183–206.
- [24] S. Wang, E. Iglesia, Experimental and Theoretical Evidence for the Reactivity of Bound Intermediates in Ketonization of Carboxylic Acids and Consequences of Acid-Base Properties of Oxide Catalysts, J. Phys. Chem. C 121 (2017) 18030– 18046
- [25] S.T. Almutairi, E.F. Kozhevnikova, I.V. Kozhevnikov, Ketonisation of acetic acid on metal oxides: Catalyst activity, stability and mechanistic insights, Appl. Catal. A 565 (2018) 135–145.
- [26] O. Kresnawahjuesa, R.J. Gorte, D. White, Characterization of acylating intermediates formed on H-ZSM-5, J. Mol. Catal. A: Chem. 208 (2004) 175–185.
- [27] A. Gumidyala, T. Sooknoi, S. Crossley, Selective ketonization of acetic acid over HZSM-5: The importance of acyl species and the influence of water, J. Catal. 340 (2016) 76–84.
- [28] X. Wang, S. Ding, H. Wang, X. Liu, J. Han, Q. Ge, X. Zhu, Conversion of propionic acid and 3-pentanone to hydrocarbons on ZSM-5 catalysts: Reaction pathway and active site, Appl. Catal. A 545 (2017) 79–89.
- [29] I. Lezcano-Gonzalez, J.A. Vidal-Moya, M. Boronat, T. Blasco, A. Corma, Identification of active surface species for Friedel-Crafts acylation and Koch carbonylation reactions by in situ solid-state NMR spectroscopy, Angew. Chem. Int. Ed. 52 (2013) 5138–5141.
- [30] Y. Jiang, M. Hunger, W. Wang, On the Reactivity of Surface Methoxy Species in Acidic Zeolites, J. Am. Chem. Soc. 128 (2006) 11679–11692.
- [31] M.V. Luzgin, V.N. Romannikov, A.G. Stepanov, K.I. Zamaraev, Interaction of Olefins with Carbon Monoxide on Zeolite H-ZSM-5. NMR Observation of the Friedel—Crafts Acylation of Alkenes at Ambient Temperature, J. Am. Chem. Soc. 118 (1996) 10890–10891.
- [32] M.L. Bonati, R.W. Joyner, M. Stockenhuber, A temperature programmed desorption study of the interaction of acetic anhydride with zeolite beta (BEA), Catal. Today 81 (2003) 653.
- [33] M.L. Bonati, R.W. Joyner, G.S. Paine, M. Stockenhuber, Adsorption studies of acylation reagents and products on zeolite beta catalysts, Stud. Surf. Sci. Catal. 154C (2004) 2724.

- [34] M.L. Bonati, R.W. Joyner, M. Stockenhuber, On the mechanism of aromatic acylation over zeolites, Micropor. Mesopor. Mater. 104 (2007) 217.
- [35] D.B. Rasmussen, J.M. Christensen, B. Temel, F. Studt, P.G. Moses, J. Rossmeisl, A. Riisager, A.D. Jensen, Ketene as a Reaction Intermediate in the Carbonylation of Dimethyl Ether to Methyl Acetate over Mordenite, Angew. Chem. Int. Ed. 54 (2015) 7261–7264.
- [36] A.D. Chowdhury, J. Gascon, The Curious Case of Ketene in Zeolite Chemistry and Catalysis, Angew. Chem. Int. Ed. 57 (2018) 14982–14985.
- [37] J.A. Martens, M. Wydoodt, P. Espeel, P.A. Jacobs, Acid-catalyzed ketonization of mixtures of low carbon number carboxylic acids on zeolite H-T, Heterogeneous Catalysis and Fine Chemicals, 1993.
- [38] Y. Woo, Y. Lee, J.-W. Choi, D.J. Suh, C.-H. Lee, J.-M. Ha, M.-J. Park, Role of Anhydride in the Ketonization of Carboxylic Acid: Kinetic Study on Dimerization of Hexanoic Acid, Ind. Eng. Chem. Res. 56 (2017) 872–880.
- [39] R. Pestman, R.M. Koster, A.V. Duijne, J.A.Z. Pieterse, V. Ponec, Reactions of Carboxylic Acids on Oxides: 2 Bimolecular Reaction of Aliphatic Acids to Ketones, J. Catal. 168 (1997) 265.
- [40] N. Cherkasov, T. Vazhnova, D.B. Lukyanov, Quantitative infra-red studies of Brønsted acid sites in zeolites: Case study of the zeolite mordenite, Vib. Spectrosc. 83 (2016) 170–179.
- [41] M. Guisnet, P. Magnoux, Coking and deactivation of zeolites: Influence of the Pore Structure, Appl. Catal. 54 (1989) 1–27.
- [42] K. Cao, D. Fan, L. Li, B. Fan, L. Wang, D. Zhu, Q. Wang, P. Tian, Z. Liu, Insights into the Pyridine-Modified MOR Zeolite Catalysts for DME Carbonylation, ACS Catal, 10 (2020) 3372–3380.
- [43] Z.V. L., M.M. A., D. J., Inhomogeneity of Broensted acid sites in H-mordenite, J. Phys. Chem., 97 (1993) 5962.
- [44] E.F.M. Stockenhuber, J.A. Lercher, Brønsted Acid Site and Pore Controlled Siting of Alkane Sorption in Acidic Molecular Sieves, J. Phys. Chem. B. 101 (1997) 5414.
- [45] M. M., J. A., L.J. C., B. E., FT infrared study of Brønsted acidity of H-mordenites: Heterogeneity and effect of dealumination, Zeolites, 15 (1995) 507-516.
- [46] T. He, G. Hou, J. Li, X. Liu, S. Xu, X. Han, X. Bao, Highly selective methanol-toolefin reaction on pyridine modified H-mordenite, J. Energy Chem. 26 (2017) 354, 358
- [47] T. Tago, H. Konno, M. Sakamoto, Y. Nakasaka, T. Masuda, Selective synthesis for light olefins from acetone over ZSM-5 zeolites with nano- and macro-crystal sizes, Appl. Catal. A 403 (2011) 183–191.
- [48] A. Bhan, A.D. Allian, G.J. Sunley, D.J. Law, E. Iglesia, Specificity of Sites within Eight-Membered Ring Zeolite Channels for Carbonylation of Methyls to Acetyls, J. Am. Chem. Soc. 129 (2007) 4919–4924.

- [49] F. Jiao, X. Pan, K. Gong, Y. Chen, G. Li, X. Bao, Shape-Selective Zeolites Promote Ethylene Formation from Syngas via a Ketene Intermediate, Angew. Chem. Int. Ed. 57 (2018) 4692–4696.
- [50] M.A. Makarova, A.E. Wilson, B.J.V. Liemt, C.M.A.M. Mesters, A.W. deWinter, C. Williams, Quantification of Brønsted Acidity in Mordenites, J. Catal. 172 (1997) 170–177.
- [51] K. Yang, J. Li, X. Zhang, Z. Liu, Investigation of the coupled reaction of methyl acetate and n-hexane over HZSM-5, Chin. J. Catal. 39 (2018) 1960–1970.
- [52] T. Romotowski, J. Komorek, Some aspects of interactions of methanol acetic acid and methyl acetate with H-Na-ZSM-5, Zeolites 11 (1991).
- [53] C.A. Gaertner, J.C. Serrano-Ruiz, D.J. Braden, J.A. Dumesic, Catalytic coupling of carboxylic acids by ketonization as a processing step in biomass conversion, J. Catal. 266 (2009) 71–78.
- [54] J. Cao, S. Ding, H. Wang, J. Han, Q. Ge, X. Zhu, Conversion of C2–4 Carboxylic Acids to Hydrocarbons on HZSM-5: Effect of Carbon Chain Length, Ind. Eng. Chem. Res. 58 (2019) 10307–10316.
- [55] T. Danuthai, S. Jongpatiwut, T. Rirksomboon, S. Osuwan, D.E. Resasco, Conversion of methylesters to hydrocarbons over an H-ZSM5 zeolite catalyst, Appl. Catal. A 361 (2009) 99–105.
- [56] T.K. Phung, M.M. Carnasciali, E. Finocchio, G. Busca, Catalytic conversion of ethyl acetate over faujasite zeolites, Appl. Catal. A 470 (2014) 72–80.
- [57] T.R. Forester, R.F. Howe, In situ FTIR studies of methanol and dimethyl ether in ZSM-5, J. Am. Chem. Soc. 109 (1987) 5076–5082.
- [58] M.H. Al-Hazmi, Y. Choi, A.W. Apblett, Acetone Condensation Over Sulfated Zirconia Catalysts, Catal. Lett. 143 (2013) 705–716.
- [59] K. Zhu, J. Sun, J. Liu, L. Wang, H. Wan, J. Hu, Y. Wang, C.H.F. Peden, Z. Nie, Solvent Evaporation Assisted Preparation of Oriented Nanocrystalline Mesoporous MFI Zeolites, ACS Catal. 1 (2011) 682–690.
- [60] R.J. Clemens, Diketene, Chem. Rev. 86 (1986) 242.
- [61] M.B. Smith, J. March, March's Advanced Organic Chemistry, fifth ed., Wiley-Interscience, Canada, 2001.
- [62] T.T. Tidwell, Ketene chemistry: the second golden age, Acc. Chem. Res. 23 (1990) 273–279.
- [63] J.F. Marlier, B.A. Haptonstall, A.J. Johnson, K.A. Sackstede, Heavy atom isotope effect on the hydrazinolysis of methyl formate, J. Am. Chem. Soc. 119 (1997) 8838–8842
- [64] J.F. Marlier, N.C. Dopke, K.R. Johnstonw, T.J. Wirdzig, A heavy-atom isotope effect of hydrolysis of formamide, J. Am. Chem. Soc. 121 (1999) 4356–4363.
- [65] A. Pabis, R. Kaminski, G. Ciepielowski, S. Jankowski, P. Paneth, Measurements of heavy-atom isotope effects using <sup>1</sup>H NMR spectroscopy, J. Org. Chem. 76 (2011) 8033–8035.